Micromechanics for energy generation

OPEN ACCESS
IOP Publishing
Journal of Micromechanics and Microengineering
J. Micromech. Microeng. **31** (2021) 114003 (18pp)
https://doi.org/10.1088/1361-6439/ac2a52

Micromechanics for energy generation

Michail E Kiziroglou[1,2] **and Eric M Yeatman**[1,*]

[1] Imperial College London, United Kingdom
[2] International Hellenic University, Greece

E-mail: e.yeatman@imperial.ac.uk

Received 16 April 2021, revised 30 June 2021
Accepted for publication 27 September 2021
Published 13 October 2021

Abstract

The emergence and evolution of energy micro-generators during the last 2 decades has delivered a wealth of energy harvesting powering solutions, with the capability of exploiting a wide range of motion types, from impulse and low frequency irregular human motion, to broadband vibrations and ultrasonic waves. It has also created a wide background of engineering energy microsytems, including fabrication methods, system concepts and optimal functionality. This overview presents a simple description of the main transduction mechanisms employed, namely the piezoelectric, electrostatic, electromagnetic and triboelectric harvesting concepts. A separate discussion of the mechanical structures used as motion translators is presented, including the employment of a proof mass, cantilever beams, the role of resonance, unimorph structures and linear/rotational motion translators. At the mechanical-to-electrical interface, the concepts of impedance matching, pre-biasing and synchronised switching are summarised. The separate treatment of these three components of energy microgenerators allows the selection and combination of different operating concepts, their co-design towards overall system level optimisation, but also towards the generalisation of specific approaches, and the emergence of new functional concepts. Industrial adoption of energy micro-generators as autonomous power sources requires functionality beyond the narrow environmental conditions typically required by the current state-of-art. In this direction, the evolution of broadband electromechanical oscillators and the combination of environmental harvesting with power transfer operating schemes could unlock a widespread use of micro-generation in microsystems such as micro-sensors and micro-actuators.

Keywords: MEMS, energy harvesting, piezoelectric, electrostatic, electromagnetic, triboelectric, energy autonomy

(Some figures may appear in colour only in the online journal)

1. Introduction

Micromechanics emerged starting in the late 1970s from two main sources—ever increasing miniaturisation of precision mechanics, for example in robotics; and the emergence of micromechanical structures fabricated using the methods and tools of integrated microelectronics. The latter, now generally known as MEMS (micro-electro-mechanical systems), soon found applications in sensing—particularly inertial sensors (accelerometers and gyros)—as well as optics (multi-mirror displays, photonic devices), microfluidics (lab-on-chip, ink-jet printer heads), and other fields. Interest soon emerged in developing electrical micro-generators in micro-mechanics, particularly to help achieve full autonomy for the increasing range of electronic devices with wireless communications, by relieving them of the constraints of batteries.

The first examples were in miniature conventional mechanics, rather than MEMS, and used two types of energy source. Direct impact devices were developed for use in shoes [1]—although these are not well suited to a high degree of miniaturisation, and there are few locations where suitable forces

* Author to whom any correspondence should be addressed.

are available, they did illustrate the advantages of piezoelectric over electromagnetic transduction in small scale generators. Inertial devices, on the other hand, use the relative motion of a sprung proof mass attached to a moving housing, and thus in principle are adaptable to any application where attachment to a moving structure is possible, and have no fundamental limit to miniaturisation (although the power output will scale accordingly). Early devices were also miniature mechanics rather than MEMS, and also used piezoelectrics (e.g. [2]). These inertial energy harvesters have essentially the same structure as accelerometers, and consequently there was early interest in developing a true MEMS harvester based on the very successful accelerometer designs.

Most early MEMS energy harvesters used electrostatic transduction, as this avoids the need for non-standard (particularly piezoelectric or magnetic) materials in the CMOS-like process. A working MEMS electrostatic harvester was demonstrated by Mitcheson *et al* [3] that used out-of-plane motion of a silicon proof mass to produce output power in the form of high voltage impulses. Power output was limited by the low mass and short internal travel distance, and these have continued to be a barrier to the success of fully MEMS inertial generators, leading many researchers to adopt a hybrid approach. Subsequently an enormous range of miniature mechanical power generators have been developed, using a wide range of structures, materials, and transduction methods. Recent reviews of piezoelectric [4–6], electromagnetic [7] and electrostatic [8, 9] energy harvesters can be found in the literature. Both direct force and inertial devices continue to be widely investigated, and a diverse range of applications have been targeted. While fully micromechanical (i.e. MEMS) remain in the minority, there has been progress in this area, and many other devices contain micro-scale (or even nano-scale) components and features.

This paper will primarily review miniature devices for generation of electrical power from ambient motion and vibration, with some comments on other applications of micro-mechanics in what could broadly be termed energy devices. The objective is to provide a simple description of the operation principles employed by these devices, including updated models that can be used instructively for understanding the key concepts, features, limitations and potential of each.

For this purpose, microgenerator devices are studied as a combination of a motion translation structure, a transducing material and a power management circuit. This approach is illustrated in figure 1. Separate analysis of each function can be beneficial in identifying possible combinations of techniques that are conventionally regarded as relevant to only a particular device type. It also helps in obtaining a generalised validity of physical and mathematical concepts.

The piezoelectric, electrostatic, electromagnetic and triboelectric transduction mechanisms are discussed in section 2. The use of a proof mass, cantilever beam, unimorphs/bimorphs and linear/rotational motion translation structures and the role and limitations of mechanical resonance are discussed in section 3. The mechanical–electrical interface, including impedance matching and active driving techniques is overviewed in section 4. Finally, alternative concepts and topics of special interest for upcoming microgenerator systems are discussed in section 5.

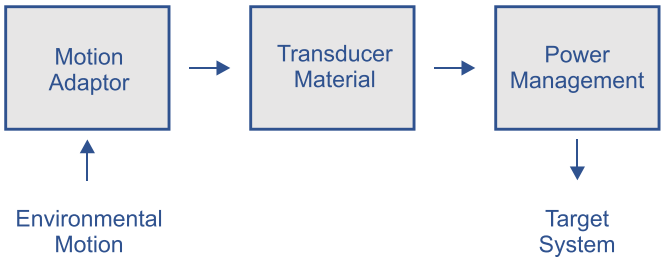

Figure 1. Functional block diagram of motion microgenerators.

2. Transduction mechanisms

MEMS devices typically involve transduction from mechanical to electrical form for generators and sensors, and vice versa for actuators and motors. The active material properties regularly employed include piezoelectricity, dielectrics and ferroelectricity, ferromagnetism for inductive transduction and triboelectricity. The corresponding mechanisms are overviewed in this section, including commonly employed materials and their relevant properties.

2.1. The piezoelectric mechanism

Piezoelectricity is the electromechanical coupling between stress T, strain S, electric field E and surface charge density D (displacement) of a bulk material. The change of inter-atomic distances in a strained dielectric material with certain crystal asymmetries can result in changes of dipole distribution. This results in material polarisation P and a corresponding surface charge $Q = P\,A$, where A is the surface area. Normal and shear strain on each direction can result in polarisation in all three dimensions. The relation between applied T and resulting P can be approximated as linear, with a tensor factor d:

$$P = d \cdot T. \tag{1}$$

The tensor d is a matrix of real numbers. For example, d_{31} corresponds to the piezoelectric constant linking the polarisation induced in direction 3, P_3 with a stress applied in direction 1, T_1. In several practical cases for a given selected input-output pair of stress and polarisation axes, the use of a single effective d-value can be used, although such a value may vary for different boundary conditions in other directions. If electrodes are deposited on two back-to-back surfaces of a piezoelectric material a capacitor C is formed. Stress driven polarisation moves charge Q to and from the electrodes. Hence, a piezoelectric generator can be modelled as a current source in parallel with a capacitor C. The dielectric (shunt) leakage and series resistance can also be included in such a model by adding corresponding components. The mechanical behaviour of the structure can be modelled with lumped

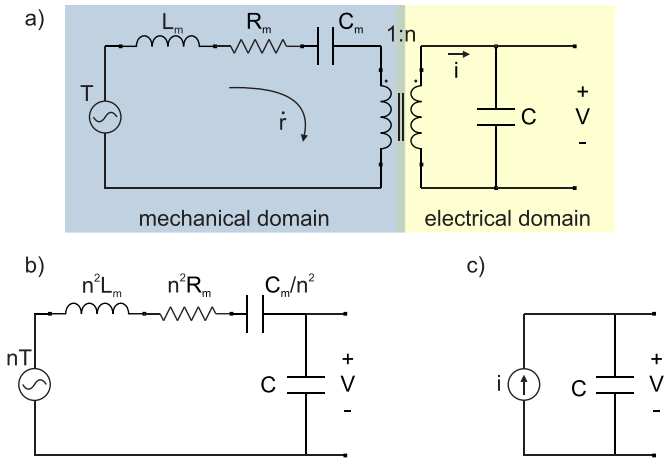

Figure 2. (a) Lumped element model of a piezoelectric generator. (b) Corresponding all-electrical model. (c) Simplified model encompassing the excitation source and mechanical response into a current source.

elements. The link between the electrical and the mechanical domain can be represented by a transformer, leading to equivalent circuits such as the one shown in figure 2(a) [10]. In this example, force is represented as a potential quantity, analogous to voltage, while mass displacement rate $\dot{r}$ is represented as a flow quantity, analogous to current. In this way, the inductance L_m, resistance R_m and capacitance C_m represent the structure mass (inertia), mechanical losses and elasticity respectively. The transformer ratio n translates force to voltage and $1/n$ translates displacement rate to current, and its units are therefore V/N or equivalently C/m.

Using circuit analysis, the mechanical components can be transferred to the electrical side as shown in figure 2(b). This model can be used to analyse the electromechanical behaviour of piezoelectric transducers. The determination of inductance L_m, resistance R_m and capacitance C_m depends on the mechanical properties and geometry of the piezoelectric material and any moving device structure to which it is attached. For bulk piezoelectric transducers such as in acoustic devices, the parameter values are primarily determined by the piezoelectric itself, while for devices such as accelerometers where the piezoelectric material forms just a small part of the moving structure, they are determined by the mechanical properties of the overall structure. An example is the typical unimorph structure, which is analysed in section 3.4.

If the electro-mechanical coupling is weak, as is generally the case, then the electrical load has little effect on the behaviour in the mechanical domain.

Consequently, maximising output power requires operation at the resonant frequency of the mechanical system, resulting in an equivalent circuit which can be modelled as a current source with a parallel capacitor C as shown in figure 2(c) (or equivalently a voltage source with series capacitor C). Note that in these models C corresponds to the capacitor formed by the piezoelectric material and its electrodes. Weak coupling also makes compensating the electrical capacitance on the mechanical side impractical. If the coupling factor could be strengthened sufficiently, this would not only allow higher power to be obtained, but would also enable tuning of the mechanical resonance using reactive components in the electrical load, as has been done with electromagnetic harvesters [11].

Table 1. Summary of common piezoelectric materials.

Material	d_{33} (nC N^{-1})	d_{31} (nC N^{-1})	References
PZT	0.63	−0.28	[12]
PMN-PT	1.25	−0.15	[13]
PNN-PZT	1.75	−0.44	[14]
$LiNbO_3$	0.006	−0.001	[15]
AlN	0.004	−0.002	[16]
PVDF	0.02	−0.015	[17]
KNN–BNZ–AS–Fe	0.5	—	[18]

The conventional general formulation of piezoelectricity is based on the following two constituent equations:

$$S = sT + d^{\mathrm{t}}E$$

$$D = dT + \varepsilon E, \tag{2}$$

where s and ε are the matrix material compliance at zero-field and electric permittivity at zero-stress respectively and d is the piezoelectric coupling matrix, with its transposition denoted as d^{t}.

A list of piezoelectric materials typically employed for energy applications is presented in table 1. The most common is lead zirconate titanate (PZT) which exhibits a d_{33} of around 0.63 nCb N^{-1}, one of the highest available in the market [12]. Single-crystal piezoelectrics employ the electrostrictive (relaxor) effect and can exhibit higher d values. The typical lead magnesium niobate-lead titanate (PMN-PT) exhibits constants higher than 1 nCb N^{-1} in single crystal form, e.g. 1.25 nCb N^{-1} in [13]. Another electrostrictive (relaxor) nickel–niobium–lead–zirconate–titanate compound, $0.1Pb(Ni_{1/3}Nb_{2/3})O_3$-$0.9Pb(Zr_{0.42}Ti_{0.58})O_3$, coined PNN-PZT, shows a d_{33} of 1.75 nCb N^{-1} in ceramic form [14]. The electrostrictive type materials are usually more challenging to use because of the high cost of single crystal and the requirement for an additional polarisation field for the electrostrictive operation principle. In microgenerators, piezoelectric materials are usually integrated in bimorph structures, exploiting their d_{31} coefficient which is smaller than d_{33}.

The use of Pb-free materials that are friendlier to the environment has also been considered, mainly using lithium niobate compounds. In [19], a potassium lithium tantalate niobate d_{33} of 0.6 nCb N^{-1} was reported, while in [20] a 46 mm^2 $LiNbO_3$ active material is used in an piezoelectric generator, demonstrating 0.38 mW from a 34 m s^{-2}, 1.1 kHz excitation. AlN has also been employed and although it offers a low piezoelectric coefficient, it is more practical to deposit and integrate in a microfabrication process. An integrated AlN harvester

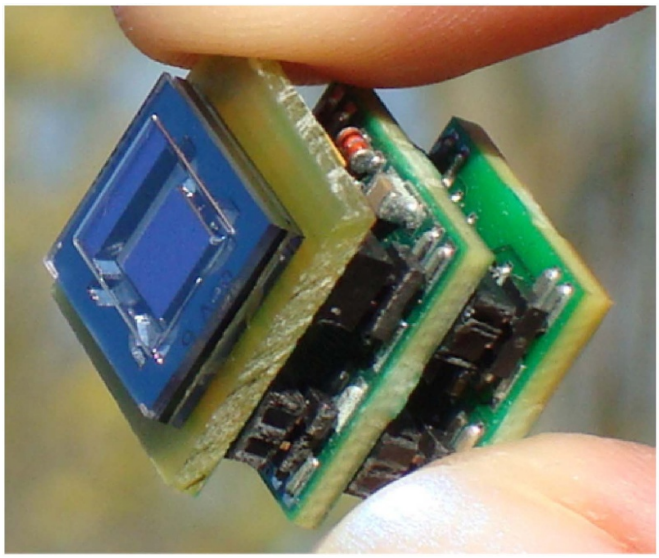

Figure 3. Energy autonomous wireless sensor powered by a 85 μW AlN piezoelectric beam harvester from a 325 Hz, 1.75 g vibration. By Elfrink *et al*, reproduced from [21]. © IOP Publishing Ltd. All rights reserved.

powering a wireless sensor has been developed by Elfrink *et al*, demonstrating 85 μW of harvested power from 325 Hz, 1.75 g vibration [21]. A photograph of the complete system is shown in figure 3.

Another important challenge is that ceramic piezoelectrics are typically fragile, brittle and very hard. The latter results in an elasticity mismatch with common structural materials for micro-mechanics such as silicon, which reduces motion, vibration or mechanical wave coupling to the environment. High elasticity is also critical for applications involving large motion displacement. Therefore, flexible piezoelectric materials are of special importance, even at a lower piezoelectric coefficient range.

A typical example is poly-vinylidene-fluoride (PVDF), which offers 0.02 and 0.03 nC N^{-1} [17, 22] in its β-PVDF isomer but with large strain capability. The combination of stiff and flexible materials has lead to a class of piezoelectrics called macro fibre composites (MFC). The structure of PVDF and MFC materials is illustrated in figure 4. Piezoelectric nanowires have also been proposed in recent years, with promising performance capabilities. Nanowire materials include PZT [23] and ZnO [24]. A variety of challenges such as device mass production, packaging and reliability have proven challenging, making commercial energy harvesting from nanowires a longer term prospect. A different type of flexible, Pb-free piezoelectric material has been proposed recently, based on KNN-BNZ-AS-Fe ceramic particles in a polydimethylsiloxane (PDMS) flexible layer, showing a d of 0.5 nC N^{-1}, integrated into a piezoelectric energy harvesting device [18].

These piezoelectric materials are typically used as active layers in beam structures, accompanied with a proof mass. These structures and their key features are discussed in section 3 of this manuscript. A review of piezoelectric energy harvesting devices can be found in [5].

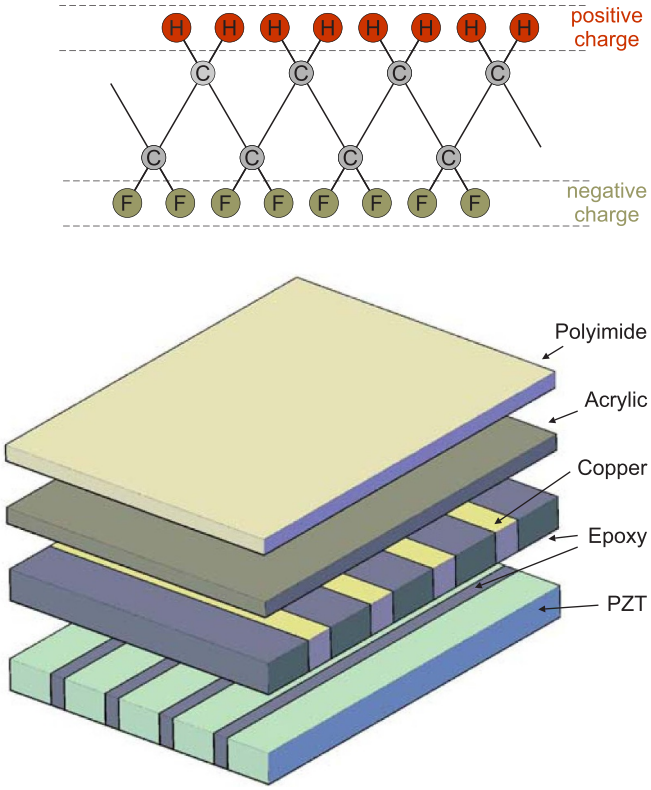

Figure 4. Top: PVDF polarisation. Bottom: MFC structure.

2.2. *The electrostatic mechanism*

Electrostatic transducers convert energy between kinetic and electrical form through the electrostatic force between charged bodies. This approach is especially well suited to MEMS, because it can be implemented in many cases with standard MEMS materials, and is easily adapted to a quasi-2D design. The similarity in structure to accelerometers is also an advantage. Consequently, most true MEMS energy harvesters are electrostatic in operation. This mechanism is typically described using the example of two charged parallel plates which can move with respect to each other, as shown in figure 5. For a given system capacitance C and initial charge Q, the electrostatic force $F_{\mathrm{T,es}}$ between the plates is [25]:

$$F_{\mathrm{T,es}} = \frac{Q^2}{2 \cdot \varepsilon_0 \cdot \varepsilon_{\mathrm{r}} \cdot A} \tag{3}$$

where ε_0 is the electrical permittivity of free space, ε_{r} is the relative permittivity and A is the area of the plates. If one of the plates is moved perpendicularly to the plate surface so that the distance y between the plates is increased (figure 5(a)), F_{es} will produce work against the motion. This work will be stored in the capacitor as electrical energy. The same will occur if the motion is parallel to the surface of the plates. This can be understood by considering that the electric field will be rotated by this motion and that the electrostatic force is parallel to the field. A component of F_{es} in the x-direction arises, which produces work as the plate is displaced along x. The corresponding geometry is illustrated in figure 5(b).

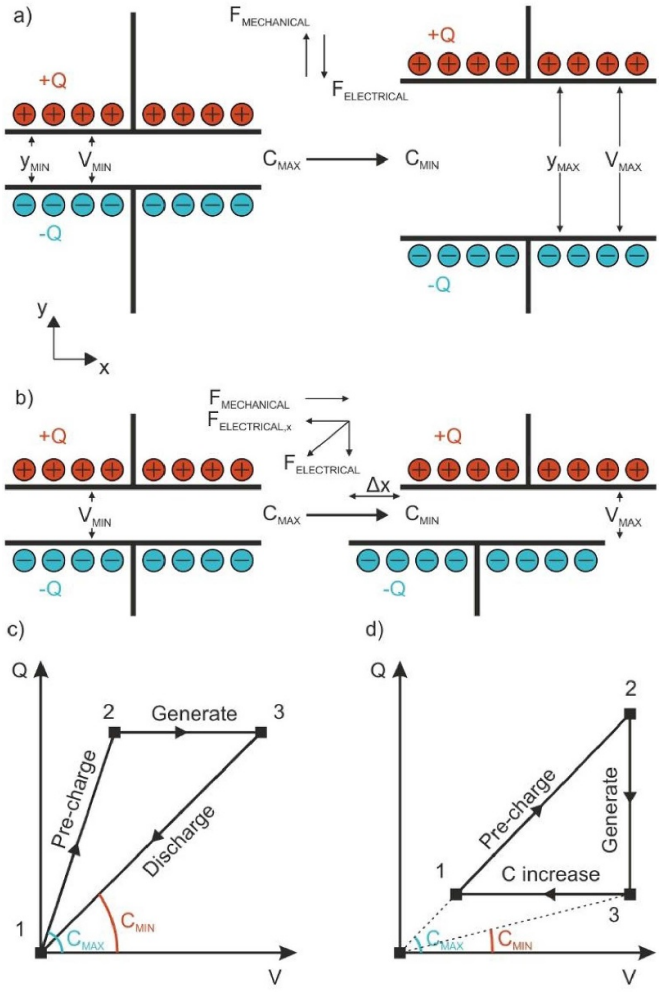

Figure 5. Electrostatic transduction with two charged parallel plates. (a) Motion perpendicular to the plates. (b) Motion in parallel with the plates. (c) Constant charge generation. (d) Constant voltage generation [26].

Effectively, if the motion results in a change of capacitance, there will be conversion between mechanical and electrical energy, as long as there is some initial charge in the system. One of the most common operational approaches is to keep a constant charge Q between the plates during motion. This can be done by charging the plates at a position of maximum capacitance $C_{\max}$ with a voltage V_{in}, supplying a charge $Q = C_{\max} V_{\text{in}}$. Capacitance decrease to a minimum $C_{\min}$ will result in voltage increase to $V_{\text{out}} = Q/C_{\min}$, and the charge Q can then be discharged at the higher voltage, thereby supplying the harvested energy. This cycle of operation is illustrated in figure 5(c). The harvested energy will be given by:

$$\Delta E_{\text{es}} = \frac{1}{2} C_{\min} {V_{\text{out}}}^2 - \frac{1}{2} C_{\max} {V_{\text{in}}}^2 = \frac{1}{2} {V_{\text{in}}}^2 \frac{C_{\max}}{C_{\min}} (C_{\max} - C_{\min}). \quad (4)$$

Another technique is to keep the voltage constant and let charge flow in or out of the plates during capacitance decrease or increase, respectively. This technique is illustrated in figure 5(d). For both cases, a general expression for the electrostatic force will be:

$$F = -\frac{\mathrm{d}E_{\text{es}}}{\mathrm{d}y} = \frac{1}{2} \cdot \frac{Q^2}{C^2} \cdot \frac{\mathrm{d}C}{\mathrm{d}y}. \quad (5)$$

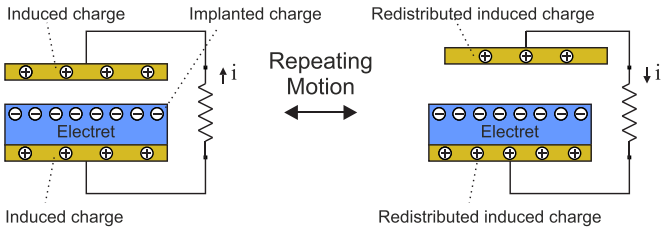

Figure 6. Operation principle of electret harvester.

As quantitatively described by equation (4), maximisation of energy per cycle of operation requires a high priming voltage, high capacitance absolute values, and a high capacitance ratio. At small scales, high capacitance values can be achieved by reducing the gap between the electrodes and by using high ε_{r} dielectrics. However, relative motion between the electrodes requires an air gap (high permittivity fluids being generally impractical), which dominates the total permittivity. For this reason, most electrostatic microgenerators use dielectrics as conventional as SiO_2. The critical factor for capacitance maximisation is the air gap size rather than the dielectric permittivity.

However, for the priming of electrostatic generators, solid state dielectrics are particularly important, as they can form electrets from which the required initial charging can be provided. Electrets are dielectrics with trapped charge that allows them to have (quasi) permanent polarisation, much like the permanent magnetism of ferromagnetic materials. The lifetime of an electret's polarisation can be 100 years.

A typical orientation for an electret-based device is shown in figure 6 [27, 28]. The electret is placed between the two capacitor plates. Its trapped charge creates an electric field which is equivalent to charging the capacitor with a high voltage (typically 100 V). Any capacitance–changing relative motion of the plates, in-plane or perpendicular-to-plane, will result in charge motion through the wires, delivering electrical energy to a load resistance R. In this operating scheme, the electret effectively provides the initial priming of the electrostatic harvesting device. Various geometrical implementations of such devices have been proposed including in-plane shifting electrodes [27], rotating electrodes [29], patterned electrodes [30] and comb-like electrode structures [31]. A quantitative analysis of operation for such devices can be found in [30]. An electret-based electrostatic microgenerator is shown in figure 7 [32]. This device employs a corona-discharge implanted CYTOP electret, a 0.1 g Si proof mass and Si-mould fabricated parylene springs, delivering 1 μW from a 2 g, 63 Hz vibration.

An overview of electret materials and their fabrication methods can be found in [9]. They involve the implantation of static charge in materials such as polytetrafluoroethylene (PTFE), CYTOP, parylene, SiO_2 and Si_3N_4. A summary of

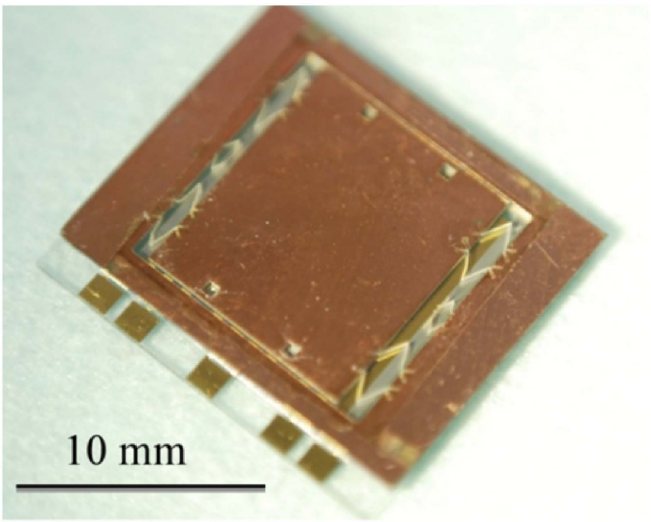

Figure 7. CYTOP electret electrostatic microgenerator by Suzuki *et al*, reproduced from [32]. © IOP Publishing Ltd. All rights reserved.

Table 2. Features of common electrets. Updated from [33].

Material	Charge density (mC m^{-2})	Deposition technique	Charge implantation technique
PTFE	0.54	Spinning	Corona discharge
CYTOP	2.5	Spinning	Corona discharge
Parylene	3.69	Room temperature CVD	Corona discharge
SiO_2/Si_3N_4	11.5	Atmospheric pressure CVD	Corona discharge

their typical features, updated from [33], is shown in table 2. Features of key importance include their surface charge density and corresponding voltage, lifetime and material/fabrication compatibility.

Ceramics in general can provide larger charge density than polymers. On the other hand, polymers are flexible and can be fabricated at lower temperature. An overview of polymer electrets can be found in [34]. The electret electrostatic harvesting concept allows the development of various motion energy generation device concepts including bistable spring structures [8], flexoelectric transduction [35], rotational harvesters for human walking [36] and their combination with switched-inductor circuit interface topologies [37].

Beyond electret-based devices, electrostatic priming can be provided by an active circuit, although a method for device initialisation is still required in this case. Another approach is the direct use of a passive sensor with voltage output as the priming source of an electrostatic harvester [38]. The main challenge of this implementation is related to the voltage range of common passive sensors which is usually lower than that required for efficient operation of electrostatic harvesters.

In electrostatic MEMS actuators, the hyperbolic increase of electrostatic field with decreasing gap distance results in an instability that causes sudden attraction to the point of minimum separation. This is called the pull-in effect and disturbs motion control for MEMS devices. In MEMS microgenerators, the induced field opposes the motion and therefore cannot lead to such an effect. However, in the potential case of using active pre-biasing techniques to increase damping in electrostatic devices, the pull-in effect should be considered. A review of pull-in instability effects for MEMS actuators can be found in [39].

2.3. The electromagnetic mechanism

In electromagnetic transducers, the effect of electromagnetic induction as described by Faraday's law is employed. Relative motion between a magnet and a coil results in magnetic flux variation which inducts an electromotive force across the coils. The motion is damped and the corresponding energy is transduced into electrical. The varying magnetic flux source an also be the field around alternating electrical currents, such as in electrical power transmission lines. In this case, the operation principle is similar to that of a transformer. Finally, electromagnetic transducers in microsystems are used in inductive and far field electromagnetic power transfer. Electromagnetic transduction is used in the vast majority of macro-scale electric generators. However, it does not scale well into the microdomain. This is due to a number of factors, including the difficulty of implementing a planar design suitable for MEMS fabrication; the difficulty of effectively guiding magnetic flux in such a planar or quasi-planar configuration; and the limited number of turns achievable in micro-scale coils, which results in low output voltages which cannot be efficiently rectified. A further challenge is heat dissipation from micro-scale coils, although this is more significant for actuators, since the power levels in energy harvesters are typically (and unfortunately) low.

For sensing applications, the design of electromagnetic transducers is oriented towards high accuracy, sensitivity, signal to noise ratio and overall optimised measurement of the effect/quantity of interest. Examples include motion, flow, proximity, sound, force, receiving antennas and others. For energy microsystems, including energy harvesters and actuators, maximum power transduction is often the priority. Consequently, a different operation point and transducer design is desirable. More specifically, coils are required to operate such that they provide maximum power and are therefore connected to impedance matched loads, instead of high impedance signal acquisition circuitry such as analogue to digital converters. In turn, this means that the coil impedance is far more important in energy microsystems than in sensing systems. This differs from the case of traditional transformers, where the power consumption at the primary coil is important and therefore transduction efficiency rather than maximum power transfer is the priority. In microsystems, power delivery is more important as the energy source is usually at macro-scale, and can be considered as effectively inexhaustible, i.e. minimally affected by the presence of the microsystem. Indeed, this complicates the discussion of 'efficiency' in micro-mechanical generators, since there is not a finite supply of power that the device seeks to convert. Instead, a measure of 'effectiveness' can be defined [40], which measures the output power as a function of input

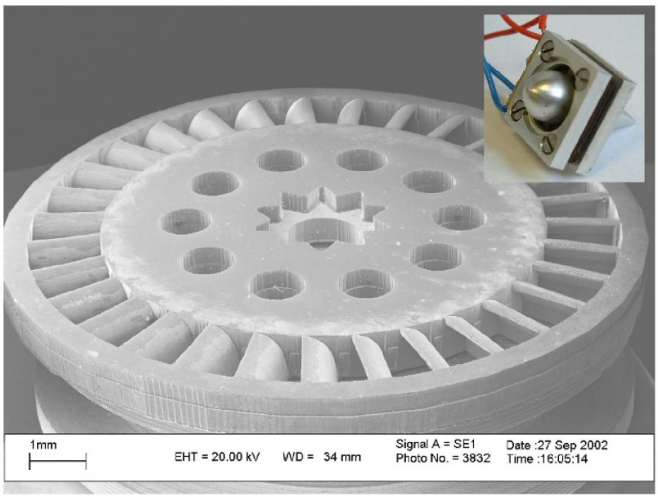

Figure 8. The rotor of a MEMS electromagnetic turbine energy harvester. The full microturbine is shown in the inset. Courtesy of A S Holmes.

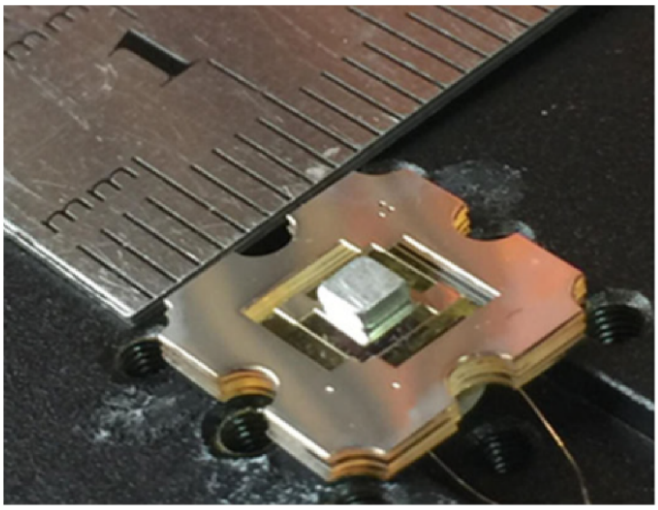

Figure 9. Vibration harvester featuring micromachined Ni springs and Cu coils, and an externally assembled 35 mg NdFeB permanent magnet. Reproduced from [56]. © IOP Publishing Ltd. All rights reserved.

motion and device size. The transducer size is generally the critical parameter for micro-generator power output for a given source. Therefore, electromagnetic microsystem transducers need to be designed for maximum power delivery per transducer mass or volume. This is also the case for many non-mechanical micro-energy sources, such as the inductive power line energy receiver introduced in [41].

Most macro-scale generators employ rotational motion, which is beneficial for generators and motors alike. In micromechanics, low loss bearings are difficult to implement, and consequently most devices use vibrating motion and flexures rather than sliding or rolling bearings. In harvesters that have rotational input motion, the rotation can be converted to oscillation via some translation mechanism. Such methods are discussed in section 3.5 of this paper.

However, high performance permanent magnets have partly tackled this challenge in particular applications such as microturbines for fluid flow [42] and rotational motion [43] energy harvesters. An SEM image of the laser micromachined SU8 rotor of a MEMS turbine by Holmes *et al* is shown in figure 8 [44].

The most common hard magnet in electromagnetic harvesters is neodymium iron boron (NdFeB), with a residual magnetic flux density between 1 T and 1.41 T, and coercivity between 760 kA m^{-1} and 1030 kA m^{-1} [45]. Samarium cobalt (SmCo) is another commercially available rare earth magnet with residual magnetic flux density between 0.83 T and 1.16 T, and coercivity between 600 kA m^{-1} and 840 kA m^{-1} [45]. NdFeB is more common due to higher strength and lower cost. On the other hand SmCo has a Curie temperature of 1000 K, significantly higher than that of NiFeB (580 K), and it is therefore preferable for high temperature applications [45].

Both NdFeB and SmCo are manufactured by sintering which involves heating a powder form of the material to high temperatures (though below the melting point), restricting their integration into MEMS design and manufacturing processes. Hence, most electromagnetic harvesters use commercially purchased and externally assembled NdFeB as permanent magnets [46–55]. Examples include both the microturbine of figure 8 and the vibration harvester presented in figure 9 [56]. The latter is based on MEMS fabricated coils and springs but it relies on manual placement for its 35 mg NdFeB permanent magnet. Reviews of various implementations, including performance comparison tables can be found in [7, 33].

MEMS integration of permanent magnets by sputtering for NdFeB and SnCo [57–59], and by electrodeposition for CoPt and FePt compounds [60–66] has been demonstrated with promising potential. The deposited materials are magnetized by the application of a strong field, which can be several Tesla, during [5] or after deposition [6]. A review of techniques for magnetic material integration into MEMS device can be found in [7].

Furthermore, the challenge of employing effective magnetic materials into micromachining processes has still limited the flux density availability. In addition, the environmental flux available in the small scale is still fundamentally limited. To address this challenge, the use of soft magnetic materials with high magnetic permeability as flux guides has the potential of achieving high flux densities in microsystems. Geometrical structures such as flux funnels have been proposed for millimetre-scale transducers demonstrating flux density amplification in the ten-to-one range [67]. An example case is the power line magnetic field energy harvesting power supply shown in figure 9 [41]. Integrating high permeability materials into microfabrication processes may enable high performance electromagnetic micro-transducers for energy as well as sensing and actuating microsystems in the near future. Candidate materials include conventional ferrites, nanocrystalline structures, ferrite films [68] as well

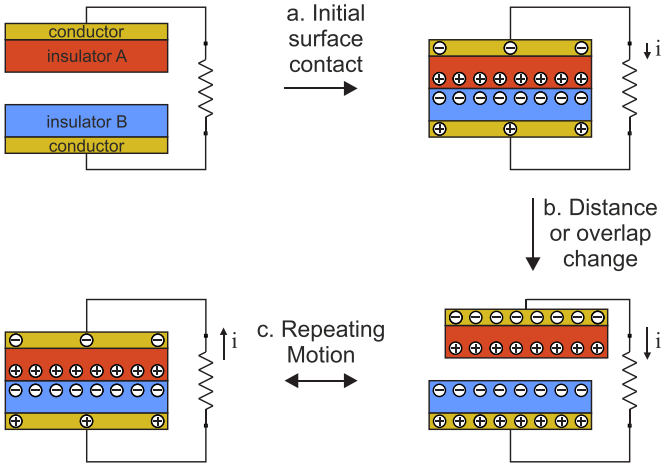

Figure 10. Operating principle of a triboelectric generator with two insulators of different electron affinities and induced charge flow on two conducting electrodes. (a) Initial contact results in charge exchange due to affinity difference. (b) Separation or reduction of overlap area leads to increased charge induction at electrodes. (c) Repeated motion leads to alternating current flow between the electrodes through an electric load.

as printable [69] and electrodeposited [70] soft magnetic materials.

2.4. The triboelectric mechanism

Triboelectricity is the effect of static charge exchange between the surfaces of two different materials when they come to contact, due to different electron energy distribution. This distribution difference is expressed as a different overall electron affinity (energy required for release from the material field). Charge accumulation depends on affinities as well as on the mechanical energy that is input for making contact and separating the two surfaces. A list of charge accumulation per Joule of contact work for different materials can be found in [71], and a systematic experimental study of charge densities using liquid mercury as a reference is reported in [72].

To form a triboelectric generator, at least one of the two surfaces is typically chosen to be insulating. Charge accumulation can then increase the electrostatic forces at the contact, thereby enhancing electromechanical coupling. The charge accumulation in the insulator is exploited inductively to move charge in conductive electrodes. The operating concept of charge induction in this orientation is similar to that of electrostatic generators. Repeated contact/separation or contact sliding modes can be implemented. A conceptual description of operation for a triboelectric generator with two insulating materials of different affinities and charge induction on two conducting electrodes is illustrated in figure 10.

The 2nd electrode can be either internal to the device, or an external environmental surface such as the human body in a so-called single-electrode operation scheme. Nanostructures are usually employed to increase contact area. A recent review of nanopatterning methods for triboelectric generators can be found in [73]. The implementation of electrodes for inductive exploitation of charge accumulation is a key element in their design [74]. Various implementations have been reported for applications including wearable microsystems [75]. A review of triboelectric nanogenerator textile technologies can be found in [76].

2.5. Comparison

The broad range of differences in prototype architecture, fabrication methods, testing conditions, and target application, makes a fair and useful comparison very difficult to achieve, especially across the transduction mechanisms. Furthermore, in most device cases functionality beyond laboratory tests and in real environments has only recently started being reported. Instead of an exhaustive figure of merit comparison, a table with three indicative implementations for piezoelectric, electrostatic an electromagnetic transduction is presented in table 3. A comparison of key features for each mechanism is presented in table 4. For state-of-the-art comparative tables the reader is referred to recent reviews [4–9].

3. Transduction structures

In the case of micromechanical generators, the environmental energy can come as a varying force applied directly on the microdevice such as a strike [78], a strain on a surface [79] or a pressure [42], as a varying force field such as an electric or magnetic field around electrical infrastructure [80], or as varying acceleration, such as vibrations or irregular human body motion [81]. In most of these cases, some kind of force or motion translation is required, from the environmental form to a form suitable for the transduction mechanism used.

The most commonly used method for coupling external acceleration to an electrostatic, piezoelectric or electromagnetic transduction mechanism is through the use of an internal proof mass which moves on a flexible suspension with respect to the device frame. In piezoelectric devices, this is typically combined with a unimorph, or bimorph, structure to increase the force on the active material. Furthermore, a variety of electromechanical techniques for translating motion between linear and rotational form are employed.

In the following subsections, the key features of these methods are summarised. A review of various motion translation mechanisms proposed for energy harvesting can be found in [82].

3.1. The use of a proof mass

In this concept, a proof mass that is attached to the frame such that it can move inside the device is used. An external force can be applied either directly to the proof mass or to the frame. The two device types are illustrated in figure 11. Taking the device frame as reference for motion, in the 1st case the force accelerates the proof mass, producing work which can be transduced to electrical energy. In the 2nd case the force accelerates the frame, so with respect to the frame, an inertial force appears on the proof mass. The work of this inertial force is used to

Table 3. Performance of three indicative MEMS energy harvesters.

Mechanism	Reference	Power	Proof mass	Conditions
Piezoelectric	Elfrink *et al* [21]	85 μW	0.1 g	17.5 m s^{-2}, 325 Hz
Electrostatic	Suzuki *et al* [32]	1 μW	0.1 g	20 m s^{-2}, 63 Hz
Electromagnetic	Shin *et al* [77]	165 μW	0.05 g	4 m s^{-2}, 46 Hz

Table 4. Comparison of features for microgenerators based on different transduction mechanisms. Green, amber and red indicate high, medium and low, respectively.

	Complexity				
Mechanism	Material	Structure	Circuit	Scalability	Power density
Piezoelectric	●	●	●	●	●
Non-electret electrostatic	●	●	●	●	●
Electret electrostatic	●	●	●	●	●
Electromagnetic	●	●	●	●	●
Triboelectric	●	●	●	●	●

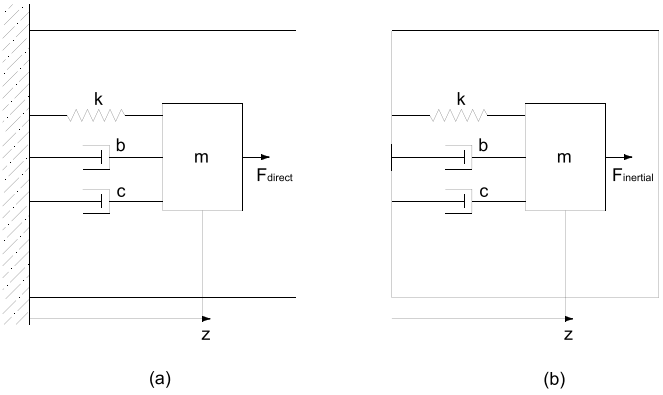

Figure 11. Typical model of a motion energy harvesting system. (a) Direct force harvester and (b) inertial force harvester.

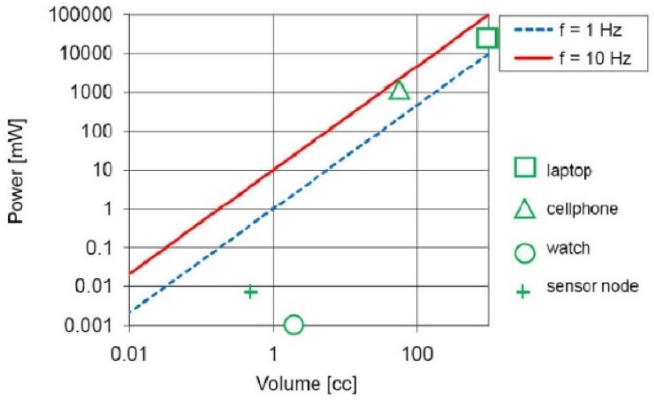

Figure 12. Maximum power for motion harvesters versus size for two different excitation frequencies, with size and power requirement of various applications superimposed [40].

transduce energy. A general formulation of equations for inertial microgenerators, including piezoelectric, electrostatic and electromagnetic transduction can be found in [33].

With a harmonic input motion but without assuming harmonic motion of the proof mass, an upper limit of the power for motion energy harvesters can be calculated as a function of device size (maximum internal displacement amplitude Z_l, mass m) and the source motion (vibration frequency ω and vibration amplitude Y_0) [40]. The maximum force that F_T can apply is the mass m times the external acceleration $\omega^2 Y_0$, otherwise the internal motion will cease. The energy extracted is this force times the internal displacement $2Z_l$, and this can be obtained twice (once in each direction) for each period $T = 2\pi/\omega$, giving a maximum power:

$$P_{max} = \frac{2}{\pi} Y_0 Z_l \omega^3 m. \quad (6)$$

Using this equation, one can assess the viability of particular motion harvesting applications. Note that this is an absolute limit for inertial harvesting devices—it cannot be overcome by improved transduction methods, or by nonlinear motion structures such as frequency up-conversion methods. The only exceptions are where the input motion is rotational rather than kinematic [83]. In that case resonant rotating devices and gyroscopic devices offer potential for large power density increases, but neither has been yet demonstrated in practice.

In figure 12, the maximum power is plotted as a function of device size for frequencies in the range expected for human motion, acceleration $\omega^2 Y_0$ of 10 m s^{-2} and a proof mass density of 20 g cm^{-3} occupying half of the device volume. By comparison with the power requirements and size of a typical laptop, cellphone, watch and sensor node, one concludes that human motion harvesting is not enough for the 1st two applications, while there is substantial promise for the last two. Indeed, the watch application has already been commercialised in high volumes, and sensors powered by harvesting are becoming more common.

3.2. The cantilever beam

In sensor, actuator as well as in energy microsystems, a suspended proof mass is typically mounted to the device frame

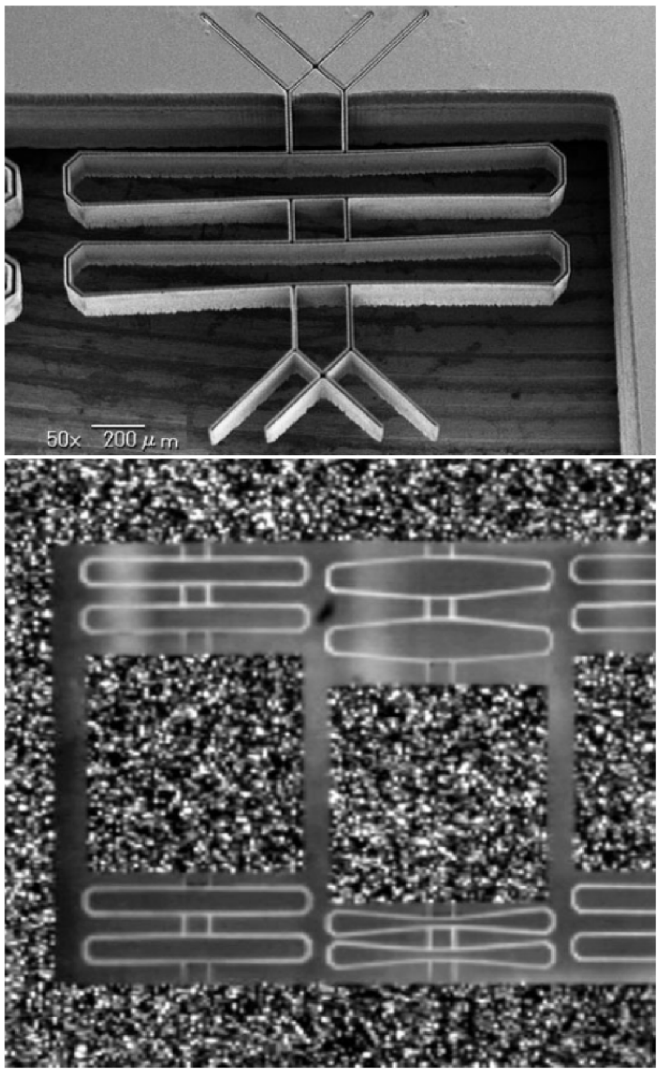

Figure 13. SEM image (top) and photograph (bottom) of parylene springs used in an electrostatic harvester, enabling a 257 Hz resonance frequency and a 0.6 mm displacement. © [2006] IEEE. Reprinted, with permission, from [86].

through a beam. The geometry of the beam is usually designed such that the desirable stiffness, motion range and damping coefficient are achieved. The ability to integrate piezoelectric materials, high capacitance and magnetic materials is of vital importance for the design of piezoelectric, electrostatic and electromagnetic transducers. For example, meander patterns can be used to increase the beam effective length, thereby reducing k and, in turn, the resonance frequency. The same patterns are also beneficial for achieving a high coupling capacitance for electrostatic devices, although additional fork-like structures are also used for this purpose. MEMS parylene springs fabricated using high aspect ratio Si moulds, used in an electrostatic device by Suzuki and Tai are shown in figure 13 [84]. An important challenge is to obtain low stiffness in the desired motion axis while maintaining high stiffness in orthogonal directions.

While such MEMS beam structures can have complicated designs, their elastic behaviour can often be calculated at 1st approximation, by considering a single cantilever beam of effective length L and rectangular cross-section $w \times t$. If E is the modulus of elasticity (Young's modulus), the longitudinal and bending stiffness can be calculated to be [85]:

$$k_{\text{longitudinal}} = E \cdot \frac{w \cdot t}{L} \tag{7}$$

$$k_{\text{rectangular}} = \frac{Ewt^3}{4L^3}. \tag{8}$$

3.3. Resonance challenges

We have seen in section 2.1 that for piezoelectric devices in particular, operation at resonant frequency can assist in coupling greater energy into the electric circuit. More generally, if the maximum internal displacement is greater than the external motion amplitude, resonance is necessary to achieve the full internal displacement range, so as to maximise power according to equation (6). This is likely to be the case only for high frequency external motion, particularly for a micromechanical device. Where the external motion amplitude is much bigger than the device dimensions, such as for human body motion, resonance does not offer this advantage. Furthermore, most ambient motion does not occur over a narrow or fixed frequency range but is broadband and stochastic in nature, which indicates that harvesting devices should be similarly broadband. Another challenge with micro-mechanical devices is that the small dimensions naturally lead to high resonance frequencies, while ambient vibrations tend to occur at low frequency (<100 Hz).

This effect can be studied by calculating the resonance frequency range for a practical set of geometrical dimensions [33]. Resonance frequency calculations as a function of beam thickness for a 10 mm long and 2 mm wide beam are shown in figure 14 for some common MEMS spring materials. A proof mass of 0.1 g was assumed corresponding to the mass of a 8000 kg m^{-3}, w-side cube. It is apparent that for low resonance frequency, beam thicknesses below 50 μm are required, even for elastic materials such as polyimide, For silicon, a beam thickness below 20 μm is needed for resonance below 10 Hz.

The effect of device scaling on resonance frequency is shown in figure 15, where a device with $w = L/5$, $\tau = L/200$ and $m = 8000$ kg m^{-3} w^3 is assumed. Proportional scaling of all dimensions leads to increase of resonance frequency. Polymers reduce the resonance frequency by an order of magnitude, but the fabrication of single beam resonators below 10 Hz at sizes smaller than 10 mm remains a challenge.

The elastic modulus and tensile strength of the spring materials that are common in energy harvesting devices are given in table 5 [33]. To achieve low resonance in the MEMS scale, suitable elastic materials could be used. PDMS has a very low Young's modulus but is viscoelastic (it behaves as a very viscous liquid), therefore it would be challenging to use

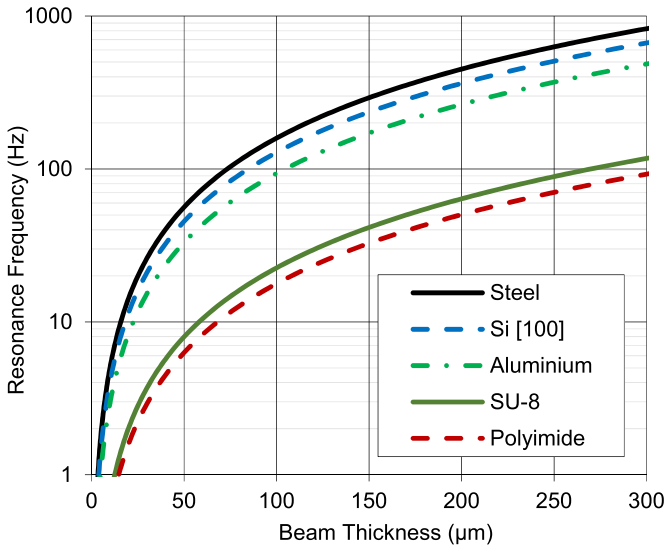

Figure 14. Beam resonance versus beam thickness calculations for a 10 mm long, 2 mm wide beam and a 0.1 g proof mass.

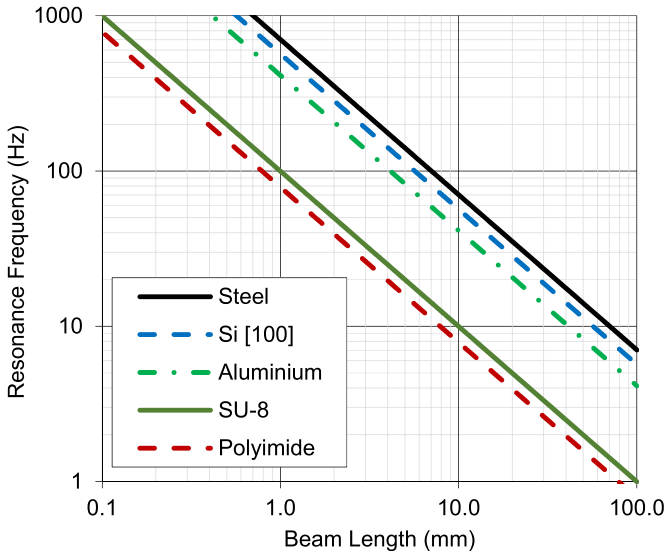

Figure 15. Calculated beam resonance for a beam with length L, width $w = L/5$, thickness $\tau = L/200$ and proof mass $m = 8000$ kg m^{-3} w^3.

in a solid state device. On the other hand, beams made by silicon nanowires exhibiting spring constants two orders of magnitude smaller than bulk silicon have been reported [87], but further k reduction and integration challenges have yet to be addressed.

Furthermore, advanced MEMS structures such as high aspect ratio, spiral and meander spring patterns [88, 89]. As well as the separate integration of a large proof mass [81] have been proposed and used. An SEM image of a 24 μm × 500 μm × 9500 μm Si spring by Pike *et al* is shown in figure 16 [89].

The possibility of eliminating the spring structure by employing a detached proof mass concept, has also been explored in which the mass can freely move by inertia inside

Table 5. Elasticity properties of materials used for MEMS springs in energy generators [33].

Material	Young's modulus (GPa)	Tensile strength (MPa)
Aluminium alloys [90]	69–73	90–570
Copper alloys [90]	130	220–1310
Stainless steel [90]	193–204	415–1790
Glass, borosilicate [90]	70	69
Silicon [111] [90, 91]	187	—
Silicon [100] [90, 92]	130	130
PMMA [90]	2.24–3.24	48–72
PET [90]	2.76–4.14	48–72
PTFE [90]	0.40–0.55	21–34
Polystyrene [90]	2.28–3.28	36–52
Polyimide [93]	2.5	230
SU-8 photoresist [93]	4.02	34
PDMS [93]	0.36–0.87 × 10^{-3}	2.24
Parylene-C [94]	3.2	70

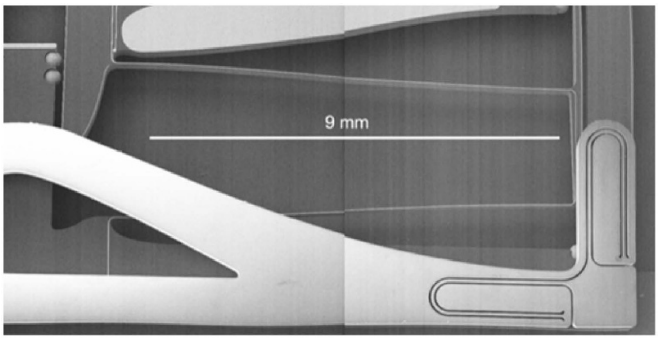

Figure 16. SEM image of high-aspect ratio Si spring enabling a very low frequency oscillator operational fabricated for a seismic sensor operating in the 0.05–10 Hz range. The spring dimensions are 24 μm × 500 μm × 9500 μm. Courtesy of W T Pike.

a container. The elimination of springs results in non-resonant devices, at the cost of energy waste as the mass hits the boundaries [38, 81]. Another approach is to use non-linear spring structures to broaden the efficient oscillation bandwidth of the micro-generator. Methods include the application of a secondary field [95], angled spring beams [96], coupling multiple springs [97], beam buckling [92], bi-stable systems [98] and the use of a sliding proof mass for self-tuning [99]. An image of a non-linear spring used in an electrostatic micro-generator by Nguyen *et al* is shown in figure 17 [96]. The beam angle results in an axial (i.e. along the beam length) stress component, which increases with displacement in one of the deflection directions (from bottom to top in figure 17). After a right-angle threshold, this stress is reversed, contributing a negative component to overall stiffness. In this way, a highly non-linear force–displacement characteristic is achieved.

Finally, so-called frequency up-conversion methods can be used to convert low frequency broadband input motion to higher frequency resonant vibration of a transducer structure such as a piezoelectric beam [100], typically using mechanical or magnetic plucking. This has the further advantage that the

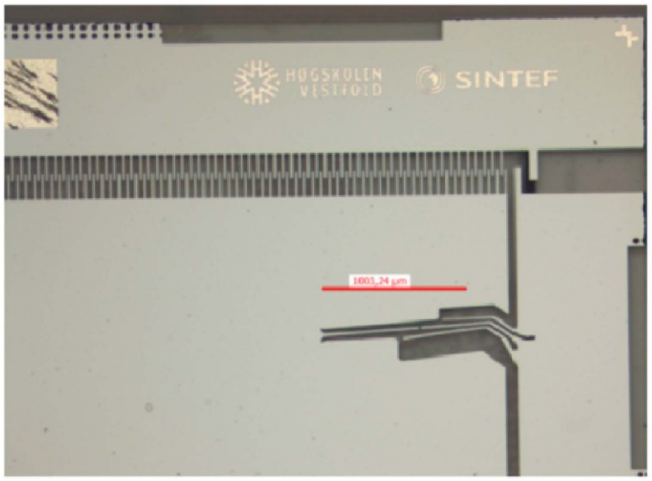

Figure 17. Non-linear spring and interleaving beams in a broadband electrostatic harvester, from Nguyen *et al*. Reproduced from [96]. © IOP Publishing Ltd. All rights reserved.

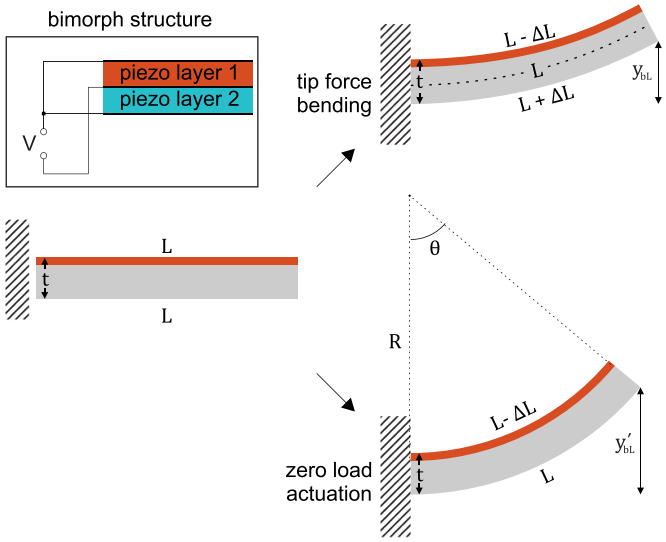

Figure 18. Geometry of a unimorph and deflection due to a force applied to its tip (right top) and due to the application of voltage (right bottom). The structure and polarisation of a bimorph is shown in the inset (left top).

input circuit can be more effectively optimised since the electrical signal is at fixed frequency. A comparative overview of frequency broadening mechanisms proposed for energy harvesting can be found in [101].

3.4. The bimorph

Bulk piezoelectric materials are usually too stiff to be used as the cantilever body. The high stiffness leads to high resonance frequency, which is usually impractical for energy generation. In addition, a large curvature leads to forces beyond fracture tolerance. For this reason, multilayer structures are typically employed, with one active and one passive, softer layer (unimorph) or two active and one passive layer (bimorph). In this way, lower total stiffness and large cantilever displacement can be achieved. The cantilever displacement is transformed to a much smaller range strain in the piezoelectric layer. The unimorph and bimorph structures are illustrated in figure 18 left and in its inset, respectively.

To calculate the relationship between the deflection of a cantilever beam y_{bL} and the longitudinal contraction of the piezoelectric layer ΔL, the cases of bending due to an external force applied at the tip, and due to an applied field in the active material are distinguished. In the 1st case, shown in figure 18 right, top, the beam shape has a polynomial form with a cubic and a quadratic term, as discussed in section 3.2. Assuming a very thin piezoelectric layer, an expression of piezoelectric contraction ΔL as a function of beam tip deflection y_{bL} can be derived:

$$\Delta L = \frac{3t}{4L} y_{bL}. \tag{9}$$

The 2nd case regards mostly actuation applications. Assuming a zero force on the cantilever tip, a piezoelectric contraction $\Delta L'$ will cause a beam arc of constant curvature and a beam tip deflection y_{bL}. Setting θ as the total arc angle, a geometrical analysis yields:

$$y'_{bL} = \frac{L\theta}{2} = \frac{L}{t}\Delta L'. \tag{10}$$

This expression is different from the 1st case of force induced deflection by a factor of 3/4, reflecting the curvature difference, but has the same geometrical dependence.

In energy harvesting, the transverse polarisation generated by the longitudinal stress of the piezoelectric is used. The material is poled such that this coupling corresponds to the d_{31} coefficient. By neglecting the effect of polarisation to the elasticity of the piezoelectric, and conversely the effect of strain to permittivity, an expression of the voltage V_c as a function of beam deflection y_{bL} can be calculated. The polarisation and the voltage will be:

$$P = d_{31}T = d_{31}E\frac{3t}{4L^2}y_{bL} \tag{11}$$

$$V = \frac{d_{31}E}{\varepsilon}\frac{3t\tau}{4L^2}y_{bL}. \tag{12}$$

In practice, the relative elasticity of the piezoelectric material, electrodes and bulk cantilever layers affect the neutral stress plane and consequently, the effective thickness t in equations (11) and (12). Therefore, while these equations are instructive on the unimorph/bimorph operation principle and design conception, detailed transducer design is typically based on finite element simulation of the coupled elasticity and piezoelectricity models, using equation (2). Interface engineering between the active and the supporting layers is key to achieving high overall transduction coupling. A review of cantilever beam piezoelectric microgenerators can be found in [5].

In actuator applications bimorphs are used to amplify the strain motion and achieve a larger actuation stroke. The geometrical gain obtained is given by equation (10). In energy

collection applications the motion translation expressed by equation (11) allows the combination of a large proof mass displacement with a large force on the piezoelectric material. This is particularly beneficial for irregular or impulse motion applications, where storing energy in mechanical oscillation form allows energy transduction by damping over multiple oscillation periods.

3.5. Translation between linear and rotational motion

A critical issue for kinematic inertial harvesters (i.e. with linear internal motion) is that the proof mass may be prevented from moving during a significant faction of time by the end-stops of its limited range. This problem can be overcome by having a rotating proof mass. This will require a bearing, and although for low-speed motion the bearing quality is less critical, this does place limits on miniaturisation and prevents a full MEMS implementation. If the centre of mass is displaced from the centre of rotation, then the mass will rotate in response to rectilinear external motion, and this is the basis of the oldest energy harvesters, the fully mechanical self-winding watches of the 19th century, with their semi-circular proof masses. More recently, such structures have been integrated with transducers to produce electrical generators. While the first of these used electromagnetic transduction, this necessitates high ratio gear trains to increase the transduction speed, in order to overcome the low voltage problem discussed above. However, the use of plucked up-conversion devices has made piezoelectric transduction practical for these harvesters, greatly decreasing device cost and complexity.

A different kind of linear motion source that is often translated into rotation is fluid flow, for which turbine mechanisms are typically employed, in combination with an inductive generator [44]. An alternative is the beam plucking mechanism [102] mentioned above. However, flow induced vibration mechanisms may also be suitable. Such mechanisms have been studied in the large scale, including pressure fluctuation [103], vortex induction [104], fluttering, buffeting and galloping devices [105, 106]. Such effects can be used for harvesting as well as flow sensing, through the vibration frequency dependence on flow speed [91, 107]. Small scale implementations are limited, but motion amplification mechanisms such as the pole-to-beam structure proposed in [108] could lead to a new range of micro-generators for fluid flow applications.

4. The mechanical–electrical interface

Apart from motion adaptors and transducer materials, micro-electromechanical energy generators also include electronic circuitry to feed the generated electrical power into the desired target system, such as a wireless microcontroller sensor. This stage is typically called power management, and it can include impedance matching, rectification, charge pumping, voltage boost or buck conversion, storage and regulation. It can also include active driving of the transducer for better performance, such as pre-biasing of piezoelectrics or synchronized switching. An analysis of the rectification and DC–DC conversion is beyond the scope of this paper, but the concepts of impedance matching, pre-biasing and the synchronized switching techniques are briefly discussed below.

4.1. Impedance matching

Because of the transient nature of ambient energy, it is important to extract the maximum power from such sources (unlike extraction from batteries, where the energy remains stored until extracted). To achieve this, a maximum power transfer operating point is often required, and an impedance matching circuit is typically used, which aims at presenting an impedance Z_L equal to the conjugate of the transducer output impedance Z_O: $Z_L = Z_O^*$. The transducer reactance must be cancelled by a load reactance of equal magnitude and opposite sign, to eliminate reactive voltage drop which otherwise reduces power transfer. In this way, the power reaching the real part of Z_O is maximised. In practice, this real part includes a voltage buck/boost converter, energy storage and the energy user system, e.g. a sensor node. The real input resistance presented by such a circuit can be dynamically controlled to match that of Z_O. This technique is called maximum power point tracking (MPPT) and can be implemented by switching an inductor between an input and a storage capacitor to achieve the desirable voltage level at the transducer input. For electromagnetic, piezoelectric and electrostatic motion transducers the real output resistance is relatively constant and therefore MPPT for the real impedance parts is often not essential. However, the reactive part is typically variable as it depends on frequency. Therefore, configurable reactive impedance matching is desirable in a wide range of energy microgenerator applications.

This method has been used to cancel the inductive output resistance of electromagnetic harvesting coils with large inductance, using tuned capacitors in series [67]. In analogy, piezoelectric transducers are capacitive and would benefit from an inductive reactance cancellation component. In energy harvesting applications, however, the operating frequency is relatively low, leading to a requirement for an impractically large inductor, e.g. 25 H for a 100 Hz motion and assuming a 100 nF transducer capacitance [109]. However, for applications involving higher frequencies, such as acoustic receivers, the approach of inductance cancellation may be interesting to explore.

4.2. Pre-biasing

In piezoelectric transducers, the coupling between an imposed strain and the generated surface charge occurring (see section 2.1) can be enhanced by the application of an additional field that opposes the development of piezoelectric charge. The charge redistribution due to strain requires more energy under such an electric field, since a higher stress is required to counter the increased electrostatic forces. This additional stress is purely coupled to the piezoelectric (i.e. geometrically asymmetric charge displacement) component of

electrostatic elasticity, and therefore it increases the piezoelectric effect.

In terms of energy transduction, the effect of pre-biasing can be analysed as an electrostatic effect, by modelling the piezoelectric material as a capacitor C with the ability to generate a piezoelectric charge $Q_P = P\,A$, where P and A are the corresponding polarisation and area, respectively. The charge Q_P is generated by a strain S in response to a stress $T = F/A$, where F is the applied force, with a piezoelectric constant d such that:

$$Q_P = d \cdot T. \tag{13}$$

For every elementary strain dS imposed, an elementary charge dQ_P is added to the capacitor. The corresponding added energy will depend on the voltage V at which this charge is brought: d$E = V$ dQ_P. This demonstrates that if a given Q_P is raised at higher voltage, by the application of an external field, an increase of energy generation is possible. The application of a given T and resulting S on the material, in the absence of initial charge, results in an energy stored in the capacitor:

$$E_1 = \frac{1}{2} Q_P V_P = \frac{Q_P^2}{2C}. \tag{14}$$

If C is pre-charged with an initial charge: $Q_E = C\,V_E$, the total energy addition by raising the additional piezoelectric charge Q_P will be equal to the energy difference between the initial and the final states:

$$E_2 = \frac{(Q_P + Q_E)^2}{2C} - \frac{Q_E^2}{2C} = \frac{Q_P^2 + 2Q_P Q_E}{2C}. \tag{15}$$

This shows that the energy gained by pre-biasing is equal to the product of the pre-biasing voltage times the polarisation charge:

$$\Delta E = \frac{Q_P Q_E}{C} = V_E Q_P. \tag{16}$$

The energy (and hence power) increase factor will be:

$$c_{PB} = \frac{E_2}{E_1} = 1 + 2\frac{Q_E}{Q_P} = 1 + 2\frac{V_E}{V_P}. \tag{17}$$

In practice, this can be implemented by charging a piezoelectric structure to a pre-biasing voltage of suitable polarity at the two displacement extremes, via a bridge of switches. Inductors are typically used for efficient charge transfer [110]. Power increase factors as high as section 4.3 have been experimentally demonstrated by this method, after accounting for pre-biasing circuitry losses [111]. Some monitoring method is needed to control switch timing, and this can be challenging if the motion is not harmonic.

The concept of improving transduction by actively applying a favourable field could be conceived also for inductive transducers. In that case, coil current flow could be actively switched through a capacitor to increase the current value at which a given magnetic flux is transduced. The employment of such a method requires further study to evaluate additional current flow losses, but could potentially be beneficial for applications involving high Q inductors.

4.3. Synchronized switch harvesting on inductor (SSHI)

Another technique to improve performance through generating piezoelectric charge at a favourable voltage is the SSHI concept introduced by Guyomar *et al* [112]. In this technique, the polarity of voltage on the piezoelectric transducer is reversed at the points of maximum strain, through an inductor that is switched accordingly. Several variants of this approach have been proposed, with some adding subsequent power processing including rectification, buck/boost conversion and voltage smoothing/regulation into the circuit design and performance analysis [113–115]. An overview and analysis of various circuit implementations has been presented in [109].

5. Other applications and trends

Although energy harvesting from ambient vibration dominates the use of micro-mechanics in power generation, there have been other types of devices investigated. A well known and early example was the MEMS gas turbine project at MIT [116]. This was a high-speed fuel-burning turbine of mm scale, with anticipated power output in the 10 W. Although fully working devices were not realised, important advances were made in design, fabrication methods (etching, wafer bonding) and high temperature materials. Another generator type which has been widely explored at the MEMS scale is the fuel cell. While fuel cells do not inherently involve motion, they may incorporate micro-mechanical components, such as pumps [117], or valves [118]. Finally, there has recently been growing interest in supplying energy to autonomous devices by acoustic power delivery (e.g. [119]). Since ultrasonic frequencies are generally used, the motion amplitudes are at the sub-micron level and the receivers are therefore solid state piezoelectric or electrostatic transducers, rather than micro-mechanical oscillators.

An important prerequisite for research and development of microsystems in general is the availability of microfabrication tools, laboratories and services accessible for research and prototyping. In previous decades, such infrastructure was provided by microelectronic research laboratories, largely supported by the CMOS industry. In recent years, the reduction of lithography resolution to the nanometre scale has restricted the interest, and hence the availability of micro-scale fabrication tools and labs. The industrial success of MEMS accelerometers led to their fast integration into CMOS motion processing units, which further contributed to prototyping restrictions. As a consequence, although microgenerator devices have shown remarkable progress in concept, their MEMS-scale implementation has seen a partial innovation plateau. On the other hand, the emergence of larger-scale prototyping techniques including additive and subtractive 3D printing, sintering and laser micromachining techniques offer new possibilities for integrated rapid prototyping of microsystems. These techniques can potentially offer a new class of prototyping tools. The increasing research and industrial interest

in micro-actuators and particularly micro-robotics is expected to support the accessibility and know-how evolution of such techniques. These developments may benefit the integration of a wide range of recently emerged microgenerator concepts into energy autonomous microsystems in the near future.

The functional description of figure 1 suggests a design approach in which different mechanical motion translation concepts are considered as a separate block that can be combined with different transduction mechanisms (active materials) and a suitable power management interface that can interact with the material or even with the mechanical structure (e.g. for switching or tuning). This offers a co-design space for overall system performance optimisation but also allows a modular route to new operating concepts and novel features. An example can be found in the employment of piezoelectric beams as MOSFET gate drivers for synchronised, active rectification of an electromagnetic energy harvesters proposed in [120].

In practice, the main limiting factor in industrial adoption of energy harvesting microsystems is the requirement for specific device designs, tailored to a very narrow set of environmental specifications, such as the availability of vibration at a specific frequency, direct sunlight or a large temperature difference across the device. This leads to a demand for customised and high cost research and development for each potential application. In spite of significant research advancement in broadening these environmental requirements, microgenerator prototypes tend to operate at lower performance in real application conditions. To address this limitation, a combination of energy harvesting and wireless power transfer could potentially be adopted. A microgenerator can be designed for off-peak normal operation within a broad environmental energy source range, providing a certain relatively low duty cycle energy autonomy level to a wireless microsystem. When required or possible, the same microgenerator can be driven to its optimum power reception point, by acoustic, vibration, inductive or optical wireless power transfer, to increase overall power autonomy reliability and predictability, or to allow reliable and practical testing of a wireless system network. This combination of energy harvesting and wireless power transfer could expand the applicability of energy autonomy to a wide range of wireless microsystems and present a promising opportunity for motion microgenerators that can exploit both resonant and off-resonance operation.

Data availability statement

All data that support the findings of this study are included within the article (and any supplementary files).

Acknowledgments

This work was partially funded by the European Commission under the H2020 Marie Sklodowska Curie ENHANCE project (Grant No: 722496).

ORCID iDs

Michail E Kiziroglou https://orcid.org/0000-0002-0165-2508
Eric M Yeatman https://orcid.org/0000-0003-0487-2693

References

[1] Kymissis J, Kendall C, Paradiso J and Gershenfeld N 1998 Parasitic power harvesting in shoes *Digest of Papers. Second Int. Symp. on Wearable Computers (Cat. No.98EX215)* pp 132–9
[2] Roundy S 2003 Energy scavenging with a focus on vibration-to-electricity conversion for low power wireless devices *PhD Thesis* University of California, Berkeley
[3] Mitcheson P D, Miao P, Stark B H, Yeatman E M, Holmes A S and Green T C 2004 MEMS electrostatic micropower generator for low frequency operation *Sens. Actuators* A **115** 523–9
[4] Liu H C, Zhong J W, Lee C, Lee S W and Lin L W 2018 A comprehensive review on piezoelectric energy harvesting technology: materials, mechanisms, and applications *Appl. Phys. Rev.* **5** 041306
[5] Safaei M, Sodano H A and Anton S R 2019 A review of energy harvesting using piezoelectric materials: state-of-the-art a decade later (2008–2018) *Smart Mater. Struct.* **28** 113001
[6] Sezer N and Koc M 2021 A comprehensive review on the state-of-the-art of piezoelectric energy harvesting *Nano Energy* **80** 105567
[7] Tan Y S, Dong Y and Wang X H 2017 Review of MEMS electromagnetic vibration energy harvester *J. Microelectromech. Syst.* **26** 1–16
[8] Murotani K and Suzuki Y 2018 MEMS electret energy harvester with embedded bistable electrostatic spring for broadband response *J. Micromech. Microeng.* **28** 104001
[9] Suzuki Y 2015 Electrostatic/electret-based harvesters *Micro Energy Harvesting* pp 149–74
[10] Roundy S and KWright P 2004 A piezoelectric vibration based generator for wireless electronics *Smart Mater. Struct.* **13** 1131–42
[11] Mitcheson P D, Toh T T, Wong K H, Burrow S G and Holmes A S 2011 Tuning the resonant frequency and damping of an electromagnetic energy harvester using power electronics *IEEE Trans. Circuits Syst.* II **58** 792–6
[12] APC International Ltd 2017 Physical and piezoelectric properties of APC materials (available at: www.americanpiezo.com/apc-materials/piezoelectric-properties.html) (Accessed 30 June 2021)
[13] He C, Zhou D, Wang F, Xu H, Lin D and Luo H 2006 Elastic, piezoelectric, and dielectric properties of tetragonal $Pb(Mg_{1/3}Nb_{2/3})O_3$–$PbTiO_3$ single crystals *J. Appl. Phys.* **100** 086107
[14] Gao X, Wu J, Yu Y, Chu Z, Shi H and Dong S 2018 Giant piezoelectric coefficients in relaxor piezoelectric ceramic PNN-PZT for vibration energy harvesting *Adv. Funct. Mater.* **28** 1706895
[15] Warner A W, Onoe M and Coquin G A 1967 Determination of elastic and piezoelectric constants for crystals in class (3 m) *J. Acoust. Soc. Am.* **42** 1223–31
[16] García J, Sanchez-Rojas J L, Ababneh A, Schmid U, González S and Iborra E 2008 Piezoelectric characterization of ain thin films on silicon substrates *XXII Eurosensors* 978-3-00-025217-4
[17] Rupitsch S J 2019 *Piezoelectric Sensors and Actuators* (Berlin: Springer) (https://doi.org/10.1007/978-3-662-57534-5)

[18] Wu M, Zheng T, Zheng H, Li J, Wang W, Zhu M, Li F, Yue G, Gu Y and Wu J 2018 High-performance piezoelectric-energy-harvester and self-powered mechanosensing using lead-free potassium–sodium niobate flexible piezoelectric composites *J. Mater. Chem.* A **6** 16439–49
[19] Li J, Li Y, Zhou Z, Guo R and Bhalla A S 2014 Piezoelectric and ferroelectric properties of lead-free niobium-rich potassium lithium tantalate niobate single crystals *Mater. Res. Bull.* **49** 206–9
[20] Clementi G *et al* 2021 $LiNbO_3$ films—a low-cost alternative lead-free piezoelectric material for vibrational energy harvesters *Mech. Syst. Signal Process.* **149** 107171
[21] Elfrink R *et al* 2010 Vacuum-packaged piezoelectric vibration energy harvesters: damping contributions and autonomy for a wireless sensor system *J. Micromech. Microeng.* **20** 104001
[22] Tichý J, Erhart J, Kittinger E and Prívratská J 2010 *Fundamentals of Piezoelectric Sensorics* (Berlin: Springer) (https://doi.org/10.1007/978-3-540-68427-5)
[23] Wu W, Bai S, Yuan M, Qin Y, Wang Z L and Jing T 2012 Lead zirconate titanate nanowire textile nanogenerator for wearable energy-harvesting and self-powered devices *ACS Nano* **6** 6231–5
[24] Qin Y, Wang X and Wang Z L 2008 Microfibre-nanowire hybrid structure for energy scavenging *Nature* **451** 809–13
[25] Zahn M *Electromagnetic Field Theory* (Massachusetts Institute of Technology: MIT OpenCourseWare) (available at: http://ocw.mit.edu) (Accessed 10 November 2011) License: Creative Commons Attribution-NonCommercial-Share Alike
[26] Mitcheson P D, Sterken T, He C, Kiziroglou E M, Yeatman A E M and Puers R 2008 Electrostatic microgenerators *Meas. Control* **41** 114–9
[27] Lo H W and Tai Y C 2008 Parylene-based electret power generators *J. Micromech. Microeng.* **18** 104006
[28] Tsutsumino T, Suzuki Y, Kasagi N and Sakane Y 2006 Seismic power generator using high-performance polymer electret *MEMS 2006: 19th IEEE Int. Conf. on Micro Electro Mechanical Systems, Technical Digest* pp 98–101
[29] Boland J, Chao Y H, Suzuki Y and Tai Y C 2003 Micro electret power generator *Mems-03: IEEE the Sixteenth Annual Int. Conf. on Micro Electro Mechanical Systems* pp 538–41
[30] Tsutsumino T, Suzuki Y and Kasagi N 2007 Electromechanical modeling of micro electret generator for energy harvesting *Transducers '07 and Eurosensors Xxi, Digest of Technical Papers, Vols 1 and 2* pp U436–7
[31] Sterken T, Fiorini P, Baert K, Puers R and Borghs G 2003 An electret-based electrostatic μ-generator *TRANSDUCERS, Solid-State Sensors, Actuators and Microsystems, 12th Int. Conf. On, 2003* vol 2 pp 1291–4
[32] Suzuki Y, Miki D, Edamoto M and Honzumi M 2010 A MEMS electret generator with electrostatic levitation for vibration-driven energy-harvesting applications *J. Micromech. Microeng.* **20** 104002
[33] Kiziroglou M E and Yeatman E M 2012 17—Materials and techniques for energy harvesting *Functional Materials for Sustainable Energy Applications* ed J A Kilner, S J Skinner, S J C Irvine and P P Edwards (Sawston, Cambridge: Woodhead Publishing) pp 541–72
[34] Li X, Wang Y, Xu M, Shi Y, Wang H, Yang X, Ying H and Zhang Q 2021 Polymer electrets and their applications *J. Appl. Polym. Sci.* **138** 50406
[35] Wen X, Li D F, Tan K, Deng Q and Shen S P 2019 Flexoelectret: an electret with a tunable flexoelectriclike response *Phys. Rev. Lett.* **122** 148001
[36] Miyoshi T, Tanaka Y and Suzuki Y 2020 Effect of natural frequency of rotational electret energy harvester for human walking *2019 19th Int. Conf. on Micro and Nanotechnology for Power Generation and Energy Conversion Applications (IEEE)* (https://doi.org/10.1109/PowerMEMS49317.2019.20515807686)
[37] Liu Y R, Badel A, Miyoshi T and Suzuki Y 2019 Dual-stage-electrode-enhanced efficient SSHI for rotational electret energy harvester *2019 20th Int. Conf. on Solid-State Sensors, Actuators and Microsystems and Eurosensors (IEEE) Xxxiii* pp 1471–4
[38] He C, Kiziroglou M E, Yates D C and Yeatman E M 2011 A MEMS self-powered sensor and RF transmission platform for WSN nodes *IEEE Sens. J.* **11** 3437–45
[39] Zhang W M, Yan H, Peng Z K and Meng G 2014 Electrostatic pull-in instability in MEMS/NEMS: a review *Sens. Actuators* A **214** 187–218 Review (in English)
[40] Mitcheson P D, Yeatman E M, Rao G K, Holmes A S and Green T C 2008 Energy harvesting from human and machine motion for wireless electronic devices *Proc. IEEE* **96** 1457–86
[41] Kiziroglou M E, Wright S W and Yeatman E M 2020 Coil and core design for inductive energy receivers *Sens. Actuators* A **313** 112206
[42] Howey D A, Bansal A and Holmes A S 2011 Design and performance of a centimetre-scale shrouded wind turbine for energy harvesting *Smart Mater. Struct.* **20** 085021
[43] Toh T, Wright S, Kiziroglou M, Mitcheson P and Yeatman E 2014 Inductive energy harvesting for rotating sensor platforms *J. Phys.: Conf. Ser.* **557** 012034
[44] Holmes A S, Hong G and Pullen K R 2005 Axial-flux permanent magnet machines for micropower generation *J. Microelectromech. Syst.* **14** 54–62
[45] 1964 Standard specifications for permanent magnet materials (available at: https://allianceorg.com/pdfs/MMPA_0100-00.pdf)
[46] Park J C and Park J Y 2011 A bulk micromachined electromagnetic micro-power generator for an ambient vibration-energy-harvesting system *J. Korean Phys. Soc.* **58** 1468–73
[47] Bouendeu E, Greiner A, Smith P J and Korvink J G 2011 A low-cost electromagnetic generator for vibration energy harvesting *IEEE Sens. J.* **11** 107–13
[48] Wang D A and Chang K H 2010 Electromagnetic energy harvesting from flow induced vibration *Microelectron. J.* **41** 356–64
[49] Yang B and Lee C 2010 Non-resonant electromagnetic wideband energy harvesting mechanism for low frequency vibrations *Microsyst. Technol.* **16** 961–6
[50] El-hami M, Glynne-Jones P, White N M, Hill M, Beeby S, James E, Brown A D and Ross J N 2001 Design and fabrication of a new vibration-based electromechanical power generator *Sens. Actuators* A **92** 335–42
[51] Saha C R, O'Donnell T, Wang N and McCloskey P 2008 Electromagnetic generator for harvesting energy from human motion *Sens. Actuators* A **147** 248–53
[52] Beeby S P, Torah R N, Tudor M J, Glynne-Jones P, O'Donnell T, Saha C R and Roy S 2007 A micro electromagnetic generator for vibration energy harvesting *J. Micromech. Microeng.* **17** 1257–65
[53] Liao L-D, Chao P C-P, Chen J-T, Chen W-D, Hsu W-H, Chiu C-W and Lin C-T 2009 A miniaturized electromagnetic generator with planar coils and its energy harvest circuit *IEEE Trans. Magn.* **45** 4621–7
[54] Beeby S P *et al* 2006 Macro and micro scale electromagnetic kinetic energy harvesting generators *DTIP 2006: Symp. on*

Design,Test, Integration and Packaging of MEMS/MOEMS 2006 pp 286–91
[55] Duffy M and Carroll D and (IEEE) 2004 Electromagnetic generators for power harvesting *Pesc 04: 2004 IEEE 35th Annual Power Electronics Specialists Conf., Vols 1–6, Conf. Proc.* (IEEE Power Electronics Specialists Conference Records) pp 2075–81
[56] Sun S, Dai X, Sun Y, Xiang X, Ding G and Zhao X 2017 MEMS-based wide-bandwidth electromagnetic energy harvester with electroplated nickel structure *J. Micromech. Microeng.* **27** 115007
[57] Budde T and Gatzen H H 2006 Thin film SmCo magnets for use in electromagnetic microactuators *J. Appl. Phys.* **99** 08N304 (in English)
[58] Walther A, Marcoux C, Desloges B, Grechishkin R, Givord D and Dempsey N M 2009 Micro-patterning of NdFeB and SmCo magnet films for integration into micro-electro-mechanical-systems *J. Magn. Magn. Mater.* **321** 590–4
[59] Jiang Y *et al* 2009 Fabrication and evaluation of NdFeB microstructures for electromagnetic energy harvesting devices *Presented at the Power MEMS* (*Washington DC*, 1–4 December)
[60] Rhen F M F, Backen E and Coey J M D 2005 Thick-film permanent magnets by membrane electrodeposition *J. Appl. Phys.* **97** 113908 (in English)
[61] Zana I, Zangari G, Park J-W and Allen M G 2004 Electrodeposited Co–Pt micron-size magnets with strong perpendicular magnetic anisotropy for MEMS applications *J. Magn. Magn. Mater.* **272** E1775–E1776
[62] Vieux-Rochaz L, Dieppedale C, Desloges B, Gamet D, Barragatti C, Rostaing H and Meunier-Carus J 2006 Electrodeposition of hard magnetic CoPtP material and integration into magnetic MEMS *J. Micromech. Microeng.* **16** 219
[63] Rhen F M F, Hinds G, O'Reilly C and Coey J M D 2003 Electrodeposited FePt films *IEEE Trans. Magn.* **39** 2699–701
[64] Pan C T, Hwang Y M, Hu H L and Liu H C 2006 Fabrication and analysis of a magnetic self-power microgenerator *J. Magn. Magn. Mater.* **304** e394–e396
[65] Wang Y Z, Jimenez B Y and Arnold D P and (IEEE) 2020 100 μm-thick high-energy-density electroplated CoPt permanent magnets *2020 33rd IEEE Int. Conf. on Micro Electro Mechanical Systems* (Proceedings IEEE Micro Electro Mechanical Systems) (NY: IEEE) pp 558–61
[66] Wang Y Z, Ewing J and Arnold D P 2019 Ultra-thick electroplated CoPt magnets for MEMS *J. Microelectromech. Syst.* **28** 311–20 (in English)
[67] Wright S W, Kiziroglou M E, Spasic S, Radosevic N and Yeatman E M 2019 Inductive energy harvesting from current-carrying structures *IEEE Sens. Lett.* **3** 1–4
[68] Ahuir J V 2021 Selection and characteristics of WE-FSFS (available at: www.we-online.com/web/en/electronic_components/produkte_pb/application_notes/auswahlundeigenschaftenvonwefsfs.php) (Accessed 30 June 2021)
[69] Peng E, Wei X, Herng T S, Garbe U, Yu D and Ding J 2017 Ferrite-based soft and hard magnetic structures by extrusion free-forming *RSC Adv.* **7** 27128–38
[70] Zong B-Y, Pong Z-W, Wu Y-P, Ho P, Qiu -J-J, Kong L-B, Wang L and Han G-C 2011 Electrodeposition of granular FeCoNi films with large permeability for microwave applications *J. Mater. Chem.* **21** 16042–8
[71] Lee B W and Orr D E The TriboElectric series (available at: www.alphalabinc.com/triboelectric-series/) (Accessed 30 June 2021)
[72] Zou H *et al* 2019 Quantifying the triboelectric series *Nat. Commun.* **10** 1427 (in English)
[73] Zou Y, Xu J, Chen K and Chen J 2021 Advances in nanostructures for high-performance triboelectric nanogenerators *Adv. Mater. Technol.* **6** 2000916
[74] Kiziroglou M E, Becker T, Yeatman E M, Schmid U, Evans J W and Wright P K 2017 Comparison of methods for static charge energy harvesting on aircraft *Microtechnologies* **10246** 102460X-102460X-6
[75] Seung W, Gupta M K, Lee K Y, Shin K-S, Lee J-H, Kim T Y, Kim S, Lin J, Kim J H and Kim S-W 2015 Nanopatterned textile-based wearable triboelectric nanogenerator *ACS Nano* **9** 3501–9
[76] Dong K, Peng X and Wang Z L 2020 Fiber/fabric-based piezoelectric and triboelectric nanogenerators for flexible/stretchable and wearable electronics and artificial intelligence *Adv. Mater.* **32** 1902549
[77] Shin A *et al* 2018 A MEMS magnetic-based vibration energy harvester *J. Phys.: Conf. Ser.* **1052** 012082
[78] Shenck N S and Paradiso J A 2001 Energy scavenging with shoe-mounted piezoelectrics *IEEE Micro* **21** 30–42
[79] Arms S W *et al* 2009 Energy harvesting wireless sensors and networked timing synchronization for aircraft structural health monitoring *Wireless Communication, Vehicular Technology, Information Theory and Aerospace and Electronic Systems Technology, 2009. Wireless VITAE 2009. 1st Int. Conf. On* pp 16–20
[80] Leland E S, Wright P K and White R M 2009 A MEMS AC current sensor for residential and commercial electricity end-use monitoring *J. Micromech. Microeng.* **19** 094018
[81] Kiziroglou M E, He C and Yeatman E M 2009 Rolling rod electrostatic microgenerator *IEEE Trans. Ind. Electron.* **56** 1101–8
[82] Zou H-X, Zhao L-C, Gao Q-H, Zuo L, Liu F-R, Tan T, Wei K-X and Zhang W-M 2019 Mechanical modulations for enhancing energy harvesting: principles, methods and applications *Appl. Energy* **255** 113871
[83] Yeatman E M 2008 Energy harvesting from motion using rotating and gyroscopic proof masses *Proc. Inst. Mech. Eng.* C **222** 27–36
[84] Fu Q and Suzuki Y 2014 MEMS vibration electret energy harvester with combined electrodes *2014 IEEE 27th Int. Conf. on Micro Electro Mechanical Systems (MEMS)* pp 409–12
[85] Kelly P A 2021 *Mechanics Lecture Notes: An Introduction to Solid Mechanics* (Auckland New Zealand: The University of Auckland) Ch 7 (available at: http://homepages.engineering.auckland.ac.nz/~pkel015/SolidMechanicsBooks/index.html) (Accessed 30 June 2021)
[86] Suzuki Y S and Tai Y 2006 Micromachined high-aspect-ratio parylene spring and its application to low-frequency accelerometers *J. Microelectromech. Syst.* **15** 1364–70
[87] San Paulo Á, Arellano N, Plaza J A, He R, Carraro C, Maboudian R, Howe R T, Bokor J and Yang P 2007 Suspended mechanical structures based on elastic silicon nanowire arrays *Nano Lett.* **7** 1100–4
[88] Ching N N H, Wong H Y, Li W J, Leong P H W and Wen Z 2002 A laser-micromachined multi-modal resonating power transducer for wireless sensing systems *Sens. Actuators* A **97–98** 685–90
[89] Pike W, Standley I, Calcutt S and Mukherjee A 2018 A broad-band silicon microseismometer with 0.25 NG/rtHz performance *2018 IEEE Micro Electro Mechanical Systems (MEMS)* pp 113–6
[90] Callister W D 1998 *Materials Science and Engineering: An Introduction* 7th edn (Wiley, New Jersey, USA.: John Wiley & Sons Inc)
[91] Kim K H and Seo Y H 2009 Self-resonant flow sensor using resonance frequency shift by flow-induced vibration *2009 IEEE 22nd Int. Conf. on Micro Electro Mechanical Systems* pp 511–4

[92] Jung S-M and Yun K-S 2010 Energy-harvesting device with mechanical frequency-up conversion mechanism for increased power efficiency and wideband operation *Appl. Phys. Lett.* **96** 111906
[93] 2012 MIT material properties database (available at: www.mit.edu/∼6.777/matprops/matprops.htm) (Accessed 30 June 2021)
[94] Selvarasah S, Li X, Busnaina A and Dokmeci M R 2010 Parylene-C passivated carbon nanotube flexible transistors *Appl. Phys. Lett.* **97** 153120
[95] Lin J-T, Lee B and Alphenaar B 2010 The magnetic coupling of a piezoelectric cantilever for enhanced energy harvesting efficiency *Smart Mater. Struct.* **19** 045012
[96] Nguyen D S Halvorsen E, Jensen G U and Vogl A 2010 Fabrication and characterization of a wideband MEMS energy harvester utilizing nonlinear springs *J. Micromech. Microeng.* **20** 125009
[97] Petropoulos T, Yeatman E M and Mitcheson P D 2004 MEMS coupled resonators for power generation and sensing *Micro Mechanics Europe* (Belgium: Leuven) 261–4
[98] Ramlan R, Brennan M, Mace B and Kovacic I 2010 Potential benefits of a non-linear stiffness in an energy harvesting device *Nonlinear Dyn.* **59** 545–58
[99] Miller L M, Pillatsch P, Halvorsen E, Wright P K, Yeatman E M and Holmes A S 2013 Experimental passive self-tuning behavior of a beam resonator with sliding proof mass *J. Sound Vib.* **332** 7142–52
[100] Renaud M, Fiorini P, van Schaijk R and van Hoof C 2009 Harvesting energy from the motion of human limbs: the design and analysis of an impact-based piezoelectric generator *Smart Mater. Struct.* **18** 035001
[101] Tao K, Tang L H, Wu J, Lye S W, Chang H L and Miao J M 2018 Investigation of multimodal electret-based MEMS energy harvester with impact-induced nonlinearity *J. Microelectromech. Syst.* **27** 276–88
[102] Fu H and Yeatman E M 2019 Rotational energy harvesting using bi-stability and frequency up-conversion for low-power sensing applications: theoretical modelling and experimental validation *Mech. Syst. Signal Process.* **125** 229–44
[103] Wang D A and Ko H H 2010 Piezoelectric energy harvesting from flow-induced vibration *J. Micromech. Microeng.* **20** 025019
[104] Li D, Wu Y, da Ronch A and Xiang J 2016 Energy harvesting by means of flow-induced vibrations on aerospace vehicles *Prog. Aerosp. Sci.* **86** 28–62
[105] Wang J L, Geng L F, Ding L, Zhu H J and Yurchenko D 2020 The state-of-the-art review on energy harvesting from flow-induced vibrations *Appl. Energy* **267** 114902
[106] Sun W P, Zhao D L, Tan T, Yan Z M, Guo P C and Luo X Q 2019 Low velocity water flow energy harvesting using vortex induced vibration and galloping *Appl. Energy* **251** 113392
[107] Shi M, Holmes A S and Yeatman E M 2020 Piezoelectric wind velocity sensor based on the variation of galloping frequency with drag force *Appl. Phys. Lett.* **116** 264101
[108] Lee Y J, Qi Y, Zhou G and Lua K B 2019 Vortex-induced vibration wind energy harvesting by piezoelectric MEMS device in formation *Sci. Rep.* **9** 20404
[109] Dicken J, Mitcheson P D, Stoianov I and Yeatman E M 2012 Power-extraction circuits for piezoelectric energy harvesters in miniature and low-power applications *IEEE Trans. Power Electron.* **27** 4514–29
[110] Dicken J, Mitcheson P D, Stoianov I and Yeatman E M 2009 Increased power output from piezoelectric energy harvesters by pre-biasing *Presented at the Power MEMS 2019* (available at: https://www.imperial.ac.uk/media/imperial-college/faculty-of-engineering/electrical-and-electronic-engineering/public/optical-and-semiconductor-devices/pubs/dicken_increased.pdf)
[111] Elliott A D T and Mitcheson P D 2012 Implementation of a single supply pre-biasing circuit for piezoelectric energy harvesters *Procedia Eng.* **47** 1311–4
[112] Guyomar D, Badel A, Lefeuvre E and Richard C 2005 Toward energy harvesting using active materials and conversion improvement by nonlinear processing *IEEE Trans. Ultrason. Ferroelectr. Freq. Control* **52** 584–95
[113] Guyomar D, Magnet C, Lefeuvre E and Richard C 2006 Nonlinear processing of the output voltage a piezoelectric transformer *IEEE Trans. Ultrason. Ferroelectr. Freq. Control* **53** 1362–75
[114] Lallart M, Garbuio L, Petit L, Richard C and Guyomar D 2008 Double synchronized switch harvesting (DSSH): a new energy harvesting scheme for efficient energy extraction *IEEE Trans. Ultrason. Ferroelectr. Freq. Control* **55** 2119–30
[115] Morel A, Pillonnet G and Badel A 2019 A tunable hybrid SSHI strategy for piezoelectric energy harvesting with enhanced off-resonance performances *J. Phys.: Conf. Ser.* **1407** 012060
[116] Epstein A H 2004 Millimeter-scale, micro-electro-mechanical systems gas turbine engines *J. Eng. Gas Turbines Power* **126** 205–26
[117] Yao S-C *et al* 2006 Micro-electro-mechanical systems (MEMS)-based micro-scale direct methanol fuel cell development *Energy* **31** 636–49
[118] Yoshida K, Tanaka S, Hagihara Y, Tomonari S and Esashi M 2010 Normally closed electrostatic microvalve with pressure balance mechanism for portable fuel cell application *Sens. Actuators* A **157** 290–8
[119] Charthad J, Weber M J, Chang T C, Saadat M and Arbabian A 2014 A mm-sized implantable device with ultrasonic energy transfer and RF data uplink for high-power applications *Proc. of the IEEE 2014 Custom Integrated Circuits Conf.* pp 1–4
[120] Lombardi G, Lallart M, Kiziroglou M E and Yeatman E M 2020 A piezoelectric self-powered active interface for AC/DC power conversion improvement of electromagnetic energy harvesting *Smart Mater. Struct.* **29** 117002